OPTWIN -A CONSTRAINED NUMERICAL OPTIMISATION METHOD FOR WING/HORIZONTAL TAILPLANE DESIGN

José Jiménez-Varona*, Angel Pascual-Fuertes
*INTA, Carretera de Ajalvir Km. 4.5, 28850 Torrejón de Ardoz, Spain

Keywords: *Design, Tailplane, Optimisation, Wing, Multidisciplinary*

Abstract

A code based on a constrained numerical optimisation method -known as OPTWIN- has been developed at INTA to address 3D aerodynamic design problems. This work is part of a national research effort partially supported by INTA to enhance its features, particularly for horizontal tailplane design problems. Multipoint design, along with geometrical and physical constraints, permits a realistic design in a multi-disciplinary environment.

A new configuration which improves a certain value function while satisfying several constraints is obtained by changing the most important geometrical features of the wing; i.e., the section geometry, chord-lengths, twist and thickness distributions, sweep angle, etc. Proper deformation functions have been implemented. Inequality constraints are implemented to fulfil several requirements, some of them of non-aerodynamic nature.

To test the capability of the code, several multipoint tailplane designs of an existing medium size transport aircraft were carried out using the OPTWIN code. Several constraints -up to nine constraints- were imposed to deal with multidisciplinary design. The designed geometries were then combined to other parts of the aircraft to take into account interference effects. The resulting configurations were later analysed with high fidelity flow solvers. The results showed that improvements of the performances of the tailplane and of the aircraft can be achieved.

1 Introduction

In the design process of an aircraft many disciplines intervene -aerodynamics, structures, controls, etc.- with complex interdependencies. In order to have appropriate tools for aircraft design it is necessary to develop multidisciplinary design tools. Efforts have been addressed in the last years to the development of multidisciplinary design optimisation tools. Good examples can be found in the literature [1, 2, 3, 4]. But, each discipline must also develop complex tools which take into account the interactions with the others. The development of optimisation tools has also been an important topic for the aerodynamicists during the last years. An extensive documentation is available. Information of some examples is given in the references [5, 6, 7, 8].

Aerodynamic design has been one of the research topics of the National Aerospace Centre of Spain -Instituto Nacional de Técnica Aeroespacial (INTA). Several codes based on inverse methods, numerical optimisation and control theory, have been developed either with its own funds or under collaborative work [9, 10, 11]. One of these codes uses as the optimiser a code based on a constrained numerical optimisation method developed by Vanderplaats [12]. The code, known as OPTWIN, has been used the last two years to address horizontal tailplane design investigation in the frame of national research. The code can cope with wing/horizontal tailplane multipoint design problems. All the

necessary requirements, constraints and value functions needed to perform the design of a new tailplane at cruise and/or low speed flow conditions, are taken into account to enhance the capabilities of the code.

In the present paper, a description of the main features of the OPTWIN code and the design procedure utilised is given, together with an example of how numerical optimisation can be used as a part of a real aerodynamic re-design of the tailplane of an existing medium size transport aircraft.

2 OPTWIN code

The OPTWIN code is a tool for wing/tailplane design which employs a constrained numerical optimisation method implemented in the CONMIN code [12] by Vanderplaats.

The OPTWIN code consists of three main modules:
1. Optimisation module
2. Flow solver module
3. Cost functions, constraints and design variables module

The optimisation module uses the method of feasible directions and is able to deal with inequality constraints.

The flow solver module employs at present two types of approach; the first one uses a viscous-inviscid interaction method based on the solution of the full potential equation and an integral boundary layer method, capable to deal with attached flow conditions. The other approach –under implementation- uses a time-accurate finite volume, cell-centered Euler code.

The third module contains the necessary information to define the cost functions, constraints and shape deformation functions which define the geometrical perturbations of the initial solution.

A more detailed description of the different modules of the code and its implementation within a design procedure follows.

2.1 Optimisation method: Feasible directions

The general optimisation problem consists of finding the design variables vector $\vec{x} = (x_1, x_2, ..., x_n)$ which minimizes an objective function of the type $f(\vec{x}) = f(x_1, x_2, ..., x_n)$ subject to a series of inequality or equality constraints:

$$g_i(\vec{x}) \leq 0 \qquad i = 1, ..., m$$
$$h_j(\vec{x}) = 0 \qquad j = 1, ..., n \qquad (1)$$

There is an initial solution of the optimal point which is modified iteratively until the conditions are fulfilled.

The general algorithm is summarized:

I. Estimate a reasonable initial solution $\vec{x}^0$

II. Compute a search direction $\vec{d}^n$. This involves the computation of the cost and constraints functions and their gradients.

III. Calculate a positive step size α_n

IV. Compute the new design as: $\vec{x}^{n+1} = \vec{x}^n + \Delta\vec{x}^n$. The superscript defines the iterative step and $\Delta\vec{x}^n = \alpha_n \cdot \vec{d}^n$ is an increment of the amount of the design variables vector.

V. Stop when converged.

The problem is then divided in two sub-problems: to find a proper step size α_n and the optimal search direction $\vec{d}^n$.

For unconstrained design problems, there are several methods to find the search directions and to compute the step size, which can be found in the literature [13].

For constrained design problems, the concept of feasible region must be introduced. The constraints bound the design space. A design, and also the starting point, can be feasible or unfeasible, depending on the fulfillment of the constraints. Additionally, in a constrained design problem, the descent function is usually

built adding to the objective function a penalty for the constraint violations.

The design direction method for constrained optimization problems implemented into the OPTWIN code is the method of feasible directions [13]. The basic idea of this method is to move from one feasible design to an 'improved' feasible design; i.e., the new design fulfils the constraints and the descent function is smaller than the old one. This method deals only with inequality constraints due to equality constraints are difficult to impose and require special procedures for their implementation.

The constraints of $g_i(\vec{x}) \leq 0$ $(i = 1,...,m)$ type can be in the following state:

- *Active constraint*. An inequality constraint $g_i(\vec{x}) \leq 0$ is said to be active (or tight) at a design point $\vec{x}^n$ if it is satisfied as an equality at this point, i.e., $g_i(\vec{x}) = 0$

- *Inactive constraint*. An inequality constraint $g_i(\vec{x}) \leq 0$ is said to be inactive at a design point $\vec{x}^n$ if it has negative value at this point, i.e., $g_i(\vec{x}) < 0$

- *Violated constraint*. An inequality constraint $g_i(\vec{x}) \leq 0$ is said to be violated at a design point $\vec{x}^n$ if it has positive value at this point, i.e., $g_i(\vec{x}) > 0$

- *ε-active constraint*. An inequality constraint $g_i(\vec{x}) \leq 0$ is said to be ε-active at a design point $\vec{x}^n$ if $g_i(\vec{x}^n) < 0$, but $g_i(\vec{x}^n) + \varepsilon \geq 0$ where $\varepsilon > 0$ is a small number. A ε-active constraint for a design point simply means that the design is arbitrarily close to a constraint boundary on the feasible side (within a so-called ε-band which can be controlled in the program by a proper parameter).

The violated constraints contribute to the definition of the descent function by means of a penalty parameter. In the OPTWIN code, this penalty parameter is introduced to be used if a design is unfeasible.

The first sub-problem is to find the improving feasible direction $\vec{d}^n$. It is a direction of descent for the cost function $f(\vec{x})$ as well as having its point on the inside of the feasible region. It can be found by:

Minimize $\nabla f(\vec{x}) \cdot \vec{d}$ subject to

$$(\nabla g_i(\vec{x})) \cdot \vec{d} \leq \Theta_i \cdot \beta$$
$$\vec{d} \cdot \vec{d} \leq 1 \qquad (2)$$

being β the maximum of $\nabla f(\vec{x}) \cdot \vec{d}$ and should be < 0. $\Theta_i > 0$ are the push-off factors, that prevent the iterations from repeatedly hitting the constraint boundary and slowing down the convergence. A value of $\Theta_i = 1$ yields acceptable results for most problems (this is introduced also as a parameter within the code). The last inequality is introduced to ensure that the search vector remains bounded.

While the program CONMIN is intended primarily to solve constrained problems, unconstrained problems may also be afforded, and the steepest descent and the conjugate direction method of Fletcher and Reeves were implemented. Later, the quasi-Newton BFGS method [14] was implemented at INTA into the CONMIN code.

2.2 Design variables

Many parameters influence the performances of a wing: the sweep angle, aspect ratio, twist distribution, wing sections…Therefore, it is very important to define as design variables the proper parameters that influence the performance such that the space design is broad enough to avoid the dependency of the solution on the initial guess. In a 3-D aerodynamic design certain flow parameters as well as geometrical parameters may be chosen as design variables. Some of them may be fixed.

In the OPTWIN code, flow parameters as the Reynolds numbers, angle of attack, etc. are fixed for each design point. A higher level of control can be exerted in the vicinity of the leading edge of the sections by using the multipoint design option. Multipoint design also allows an overall good behavior for off-design conditions.

Geometrical parameters are chosen as design variables. Modifications of the sweep angle, dihedral angle, twist distribution, chord distribution and maximum thickness distributions have been included. For the sweep and dihedral angles linear variations are implemented. For these modifications, only one design variable is needed. For the chord distribution, piecewise linear variations are allowed, in order to deal with trapezoidal wings or cranked wings. Three design variables are needed for this type of shape deformation. For the twist distribution, modifications such that one line $\left(\dfrac{x}{c}\right) = cte$ is kept linear are considered. This is useful for the hinge moment line of a tailplane. It may be of interest to avoid modifying this line becoming a curve line. Two design variables are needed.

Modifications of the shape of the wing sections using several deformation functions are also included. For this purpose, there are several deformation functions which may be implemented. In the OPTWIN code, the deformation functions included are the following:

1. NACA functions
2. Wagner functions
3. Legendre polynomials
4. Hicks-Vanderplaats functions
5. Patched polynomials
6. Bèzier curves
7. Thickness-mean line functions

The first six functions are widely described in the literature. For Bèzier curves, a method for fitting the initial sections to a set of Bèzier polynomial has been developed and implemented into the code [10]. The control points -up to 25 control points may be used to define a section- are then used as design variables. For the final list of functions, they were internally developed at INTA in order to have adequate deformation functions, especially in the leading and trailing edges. One set of basic functions for the deformation of the thickness distribution was implemented in the following form:

$$f_t(x) = 4 \cdot x^{p(x_{m_i})}\left(1 - x^{p(x_{m_i})}\right)$$

being $p(x_{m_i})$ \hfill (3)

$$p(x_{m_i}) = \frac{\log(1/2)}{\log(x_{m_i})} \qquad 0 \le x_{m_i} \le 1$$

The value x_{m_i} is the percentage of the chord where the maximum of $f_t(x)$ is located. The parameter x_{m_i} may be expressed as:

$$x_{mi} = \frac{i}{N+1} \quad i = 1,...N \qquad (4)$$

being N the number of selected functions.

For the mean line, the following functions are used:

$$f_c(x) = 4 \cdot (1-x)^{p(x_{m_i})}\left(1 - (1-x)^{p(x_{m_i})}\right)$$

being $p(x_{m_i})$ \hfill (5)

$$p(x_{m_i}) = \frac{\log(1/2)}{\log(1-x_{m_i})} \quad \text{for} \ \ 0 \le x_{m_i} \le \frac{1}{2}$$

and,

$$f_c(x) = 4 \cdot x^{p(x_{m_i})}\left(1 - x^{p(x_{m_i})}\right)$$

being $p(x_{m_i})$ \hfill (6)

$$p(x_{m_i}) = \frac{\log(1/2)}{\log(x_{m_i})} \qquad \frac{1}{2} \le x_{m_i} \le 1$$

An expression for x_{m_i} similar to that of the thickness functions may be used.

These basic functions are used as perturbation functions to the initial solution. The design variables scale the value of these functions.

The deformation of the wing section if these functions are used should be:

$$\Delta f(\vec{x}) = \sum_{i=1}^{N1} a_i \cdot f_{it}(\vec{x}) + \sum_{j=1}^{N2} b_j \cdot f_{jc}(\vec{x}) \qquad (7)$$

being the values a_i, b_j the design variables.
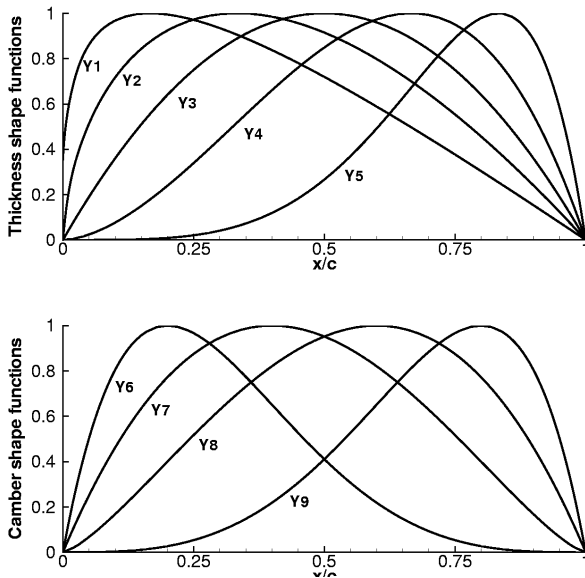
Fig. 1. Thickness and mean line shape functions.

Using these functions has proven to be very effective for the wing sections deformation, since they prevent an infinite slope at the leading edge for the mean line, and provide a more general design space than other functions [10].

Figure 1 shows these functions for a number of 5 design variables for the thickness functions and 4 design variables for the mean line functions.

This type of functions has been chosen for the test cases which will be shown in the chapter 4.

Depending on the case to be studied, the number of design variables may vary between 2-3 to a very large number (~100), if section variations are done and a large number of design variables are chosen for each section. It can be seen that an optimisation design may be time consuming. The designer must choose adequately the cost function and the number and type of design variables needed to perform

a design within a reasonable computational cost.
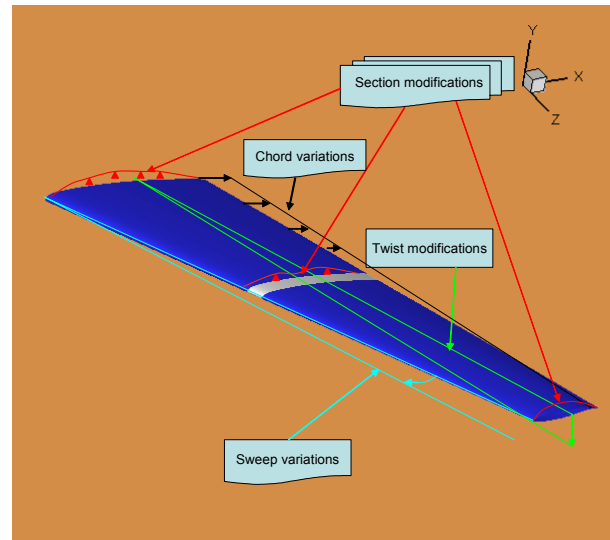
Fig. 2. Type of possible shape deformations of a wing/tailplane implemented into OPTWIN code

A schematic view of the type of shape deformations implemented into the code is given in figure 2.

2.3 Cost functions and constraints

The OPTWIN code is being developed such that a wide variety of options for the cost functions is implemented. At first, a set of cost functions based on the global aerodynamic coefficients was selected. For aerodynamic purposes, the lift, drag and pitching moment coefficients (C_L, C_D, C_M) may be combined to define cost functions to be minimised. An example is $\left(\dfrac{C_D}{C_L} \right)$ (inverse function of the aerodynamic efficiency). But, in some cases, an inverse design function of the type $f(\vec{x}) = \int_S \left(C_p - C_{pobj} \right)^2 dS$ is of interest. This function has also been implemented into the OPTWIN code.

The code is capable to perform multipoint design. Therefore, a cost function based on a combination of the cost functions at each design point is built, using proper weighting factors for each design point.

$$f(\vec{x}) = \sum_{i=1}^{n} \omega_i \cdot f_i(\vec{x}) \quad \text{with} \sum_{i=1}^{n} \omega_i = 1 \quad (8)$$

being n the number of design points. Usually, two or three design points are enough for practical designing, but it is possible to use more if necessary.

Geometric	Aerodynamic
Min/Max section area	Min/Max lift coefficient C_L
Min/Max leading edge radius	Min/Max pitching moment coefficient C_M
Min/Max trailing angle	Min/Max hinge moment coefficient Ch
Min/Max trailing edge slope	Minimum Cp
Min/Max $(t/c)_{max}$	Maximum Grad(Cp)
Min/Max (x/c) position of $(t/c)_{max}$	Maximum bending moment
Max twist	
Min/Max chord-length	

Table 1 Geometric and aerodynamic constraints implemented into the OPTWIN code.

In a multidisciplinary environment, constraints are extremely important in order to obtain realistic design shapes. A wing design code needs to count on the ability of posing constraints of different type. The OPTWIN code performs this by a set of constraints of both geometrical and aerodynamic nature. The set of constraints actually implemented is given in table 1.

The designer must have the input of other disciplines, which may be converted into a constraint, preferably a geometric or aerodynamic constraint. The OPTWIN code is continuously revised in order to implement additional constraints.

The constraints may be imposed into the code in a relatively straightforward manner, but a constrained design must be carried out using the least possible number of constraints. The feasible design region is reduced when the number of constraints is increased; and it may occur that the optimisation problem is over-constrained and therefore, there is not a feasible region. The skillness of the designer is very important to pose an optimisation problem with several constraints. On one hand, an unconstrained problem usually produces unrealistic or non-practical geometries; on the other hand, a constrained problem may not have a feasible solution if is over-constrained.

2.4 Flow solvers

The OPTWIN code has been programmed the best modular way possible in order to ease the replacement of the flow solver. Up till now, the code can use as the flow solvers two codes. The first one uses a viscous-inviscid interaction method based on the solution of the full potential equation and an integral boundary layer method (FPE+BL) capable to deal with laminar and turbulent boundary layers, using empirical transition methods [15, 16]. This code has proven to be very robust and to provide accurate solutions for designing purposes in attached flow conditions. The second code -which is currently being implemented- is a time accurate finite volume, cell-centered Euler code, which employs a central differencing with Jameson type second and fourth difference dissipation operator, and an explicit multistage Runge-Kutta scheme [17]. This code has been assessed within the V European Frame Programme project VELA (Very Efficient Large Aircraft) concerned to blended wing body aircraft.

3 Design Procedures

The OPTWIN code is a valuable tool which must be used within a design procedure capable to deal with all the necessary steps to achieve a new shape which fulfils an improvement in aerodynamic performances while maintaining some features and geometrical constraints.
Figure 3 shows a block-diagram of the design procedure utilised.
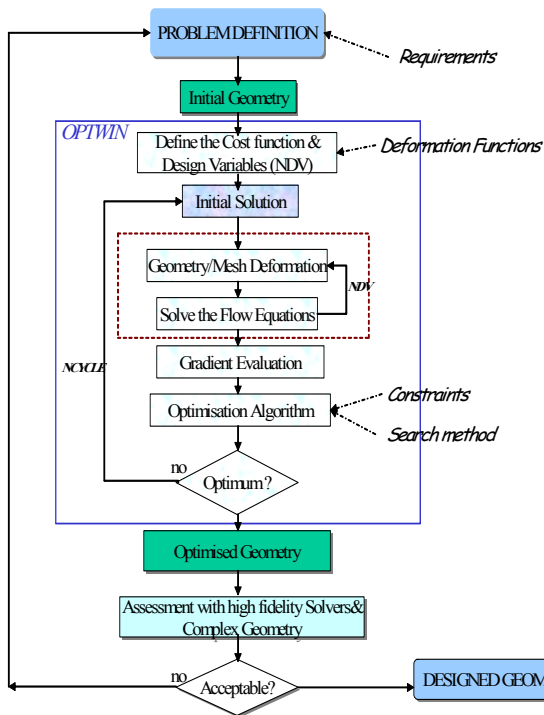
Fig. 3.Block diagram of the methodology for HTP design problems.

First, a design problem with several requirements is posed. Some of these requirements arise from non-aerodynamic considerations in order to achieve a realistic configuration. Then, the input data for the OPTWIN code are given: a cost function is chosen. Several constraints are imposed in order to ensure that the objective is achieved fulfilling the requirements. Then, the number and type of deformation functions is chosen. Several numerical parameters, as number of design cycles, penalisation parameters for the constrained problem, etc., are chosen.

The optimisation is carried out and, the optimised solution is then analysed with high fidelity flow solvers. Additionally, the configuration fuselage-horizontal tailplane or wing/fuselage is analysed in order to take into account interference effects. If the optimised solution fulfils the requirements, it is chosen as the designed geometry. In case of not achieving an acceptable solution, the design problem should be posed again. There are several possibilities: cost functions, deformation functions, design variables, constraints, etc.,

may be modified. It is up to the designer to decide how to continue by choosing the appropriate modifications in the design problem. In every design procedure it is necessary the "man-in-the-loop" presence.

It is worth to comment computing times. The number of evaluations per design point is:

$$N_{eval} = N_{design\,variables} + N_{constraints} + 1 \qquad (9)$$

The total number of evaluation of the cost function is then:

$$N_{total} = N_{design\,cycles} \cdot N_{eval} \qquad (10)$$

For the majority of cases tested up till now, the number of design variables used is about 40; it is sufficient to use 9 constraints or less. Then, a typical number of evaluations may be 50 per design cycle. A typical multipoint case is a dual-point case. Therefore, 100 evaluations may be needed for a design cycle.

Most of the test cases carried out needed 8-12 design cycles. Therefore, 1000 evaluations of the gradients are required for a typical case. The computational effort is not high when using as flow solver the full potential + B.L. method implemented in OPTWIN. The computing times of most cases were about 12 hours in a HP-Superdome with PARISC processors at 750 MHz and 24 Gb of RAM memory.

4 Tailplane Optimisation of a medium size transport aircraft

Basic research in the horizontal tailplane (HTP) design field has been done in Spain in different projects. In one of these, the development and use of numerical optimisation tools was faced with the participation of INTA. Some results and conclusions of HTP design studies are included in the present paper. It is intended to optimise an existing HTP without changing the plan form shape.

Figure 4. Detail of the aft body of a medium size transport aircraft.

Three different approaches have been undertaken in order to improve the HTP characteristics at high and low speed. The goal is to reduce the drag of an existing HTP at high-speed cruise conditions without degrading stall features at low speed and fulfilling some requirements.

4.1 Multipoint twist design at high speed and low speed

The first approach consists upon the optimisation of the span wise twist distribution at high speed and at low speed, in order to reduce the drag. Modifications in the twist distribution involve three design variables, so design results can be obtained at a low computational cost (1 or 2 hours time for HP-Superdome with PARISC processors at 750 MHz). The airfoil shapes are to be kept unchanged.

Two design points have been taken:

$M_1 = 0.78, \text{Re} = 16.9 \cdot 10^6, \alpha = -1.35^\circ \, (cruise)$

$M_2 = 0.20, \text{Re} = 12.6 \cdot 10^6, \alpha = -4.50^\circ$

(Reynolds number is based on the HTP aerodynamic mean chord AMC). The weighting factors are $\varpi_1 = 0.5$ and $\varpi_2 = 0.5$. The cost function is

$$f(\vec{x}) = \sum_{i=1}^{2} \varpi_i \cdot \left(1 - \frac{C_{D_i}}{C_{Dobji}}\right)^2 \qquad (11)$$

The value C_{Dobj} is the target C_D, which has been chosen lower than the initial value in order to obtain a cost function of order unity.

A geometrical requirement must be fulfilled:

$$Twist_{max} \leq 5^\circ \qquad (12)$$

Figure 5 shows the drag polar curves at Mach number 0.78 (the new design is referred as HTP Optimal Twist).

Mach 0.78
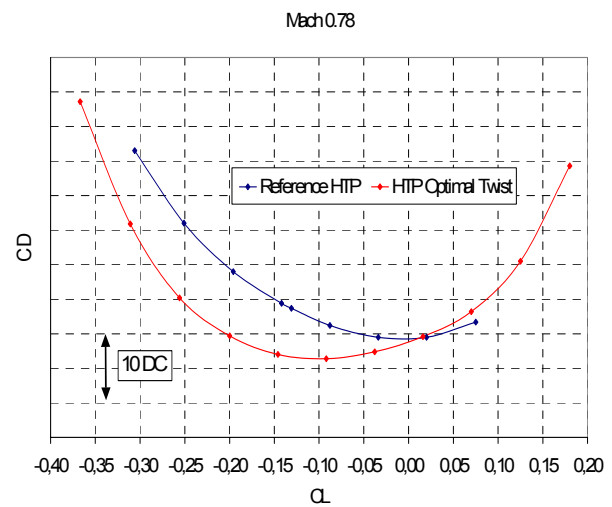
Figure 5. Drag polar comparison between the reference HTP and the HTP Optimal Twist (Reference Surface = $S_{HTP} = 31 \, m^2$).

A drag saving of 4.8 drag counts (DC) -based on the HTP reference surface- has been obtained for $C_{Lh} = -0.10$. Note that actually the drag improvements have been obtained for negative lift coefficients, where the HTP usually operates.

4.2 Multipoint design at high speed

The second approach consists in optimise the HTP aerodynamic drag at high speed, modifying the airfoil sections. A two-point problem has been posed:

$M_1 = 0.78, \text{Re} = 16.9 \cdot 10^6, \alpha = -1.45^\circ \, (cruise)$

$M_2 = 0.82, \text{Re} = 16.9 \cdot 10^6, \alpha = -1.45^\circ$

(Reynolds number is based on the HTP aerodynamic mean chord AMC). The weighting factors are $\varpi_1 = 0.5$ and $\varpi_2 = 0.5$. Transition is fixed at the leading edge to consider fully turbulent flow.

The cost function is again

$$f(\vec{x}) = \sum_{i=1}^{2} \varpi_i \cdot \left(1 - \frac{C_{D_i}}{C_{Dobji}}\right)^2 \qquad (13)$$

in order to reduce drag. The value C_{Dobj} is the target C_D.

Some geometrical and aerodynamic requirements must be fulfilled:

$$0.098 \leq \left(\frac{t}{c}\right)_{max} \leq 0.150$$

$$(R)_{le} \leq 0.0065$$

$$8.00º \leq (\Theta)_{te} \leq 16.0º \qquad (14)$$

$$C_{L1} \leq C_L \leq C_{L2}$$

$$C_{h1} \leq C_h \leq C_{h2}$$

being the values named with subscripts 1 and 2 defined values. The reference HTP has a constant airfoil shape along the span having a thickness-to-chord ratio of $\left(\frac{t}{c}\right)_m = 0.098$. By defining the optimisation problem in this way the goal is to obtain new geometries with higher thickness-to-chord ratio than the original. This is favourable in order to reduce the structural weight. The constraint in hinge moment is also imposed to preserve the low value of the reference configuration.

The HTP model is built by means of 11 sections equally spaced along the span. The modification of the sections has been introduced in three sections -root, 40% of span and tip- interpolating linearly for the sections between them. Six thickness shape functions have been taken and six camber shape functions –as defined in chapter 2.2- for any of three sections. No plan form modification has been applied, so 36 design variables are used.
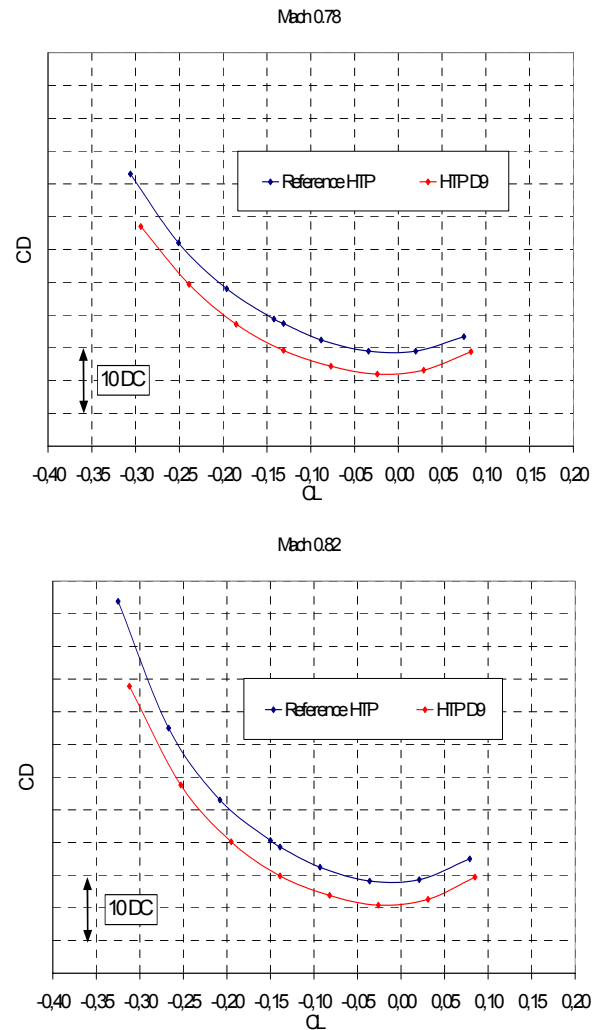
Figure 6. Drag polar comparison between the reference HTP and the HTP D9. (Reference Surface = S_{HTP} = 31 m^2).

Some new designs were obtained having a drag saving in all cases when analysed with the OPTWIN FPE+BL flow solver. The best one is named as *HTP D9*. Figure 6 presents the drag polar curves for the reference geometry and for the new design at Mach number 0.78 and 0.82.

For the design points the results predicted by OPTWIN are:

Mach number 0.78: drag saving of 4.2 DC (based on the HTP reference surface) and at the same lift coefficient:

Reference HTP:

$M_1 = 0.78, \mathrm{Re} = 16.9 \cdot 10^6, \alpha = -1.45º$

$C_L = -0.142$

HTP D9

$M_1 = 0.78, \mathrm{Re} = 16.9 \cdot 10^6, \alpha = -1.55º$

$C_L = -0.142$

Mach number 0.82: drag saving of 4.7 DC (based on the HTP reference surface) and at the same lift coefficient:

Reference HTP:

$M_2 = 0.82, \mathrm{Re} = 16.9 \cdot 10^6, \alpha = -1.45º$

$C_L = -0.150$

HTP D9

$M_2 = 0.82, \mathrm{Re} = 16.9 \cdot 10^6, \alpha = -1.56º$

$C_L = -0.150$
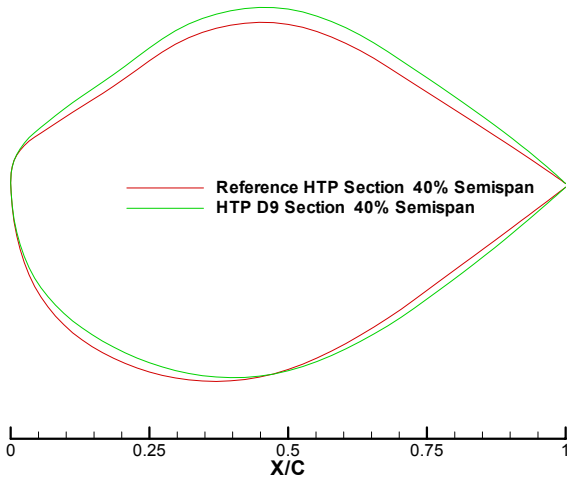
Figure 7. Initial and designed geometries (HTP D9) at span section η=0.40.

It is important to remark that drag savings were obtained by fulfilling all the requirements imposed by the constraints. The thickness-to-chord ratio of the different sections is higher than the original, leading to better structural characteristics. The hinge moment coefficient has been reduced about a 50%, leading to a weight saving in the elevator actuators and power needs.

Figure 7 shows the comparison of the geometries of the initial and designed 40% semi-span sections. It may be noticed the increment in thickness-to-chord ratio.

4.3 Multipoint design at high speed and low speed

The third approach tries to optimise the HTP drag at high speed, limiting Cp peak at low speed regime, in order to also improve the low speed stall behaviour. The airfoils shape modifications are made in a similar way than for the previous test case. It is worth noting that usually the HTP low speed characteristics determine the tail sizing, especially the negative stall angle. The two-point design problem is posed at:

$M_1 = 0.78, \mathrm{Re} = 16.9 \cdot 10^6, \alpha = -1.45º \ (cruise)$

$M_2 = 0.20, \mathrm{Re} = 12.6 \cdot 10^6, \alpha = -4.00º$

The cost function is the same than that used in the previous test case; but, the weighting factors are $\varpi_1 = 0.9$ and $\varpi_2 = 0.1$.

Some geometrical and aerodynamic requirements must be fulfilled:

$$0.098 \leq \left(\frac{t}{c}\right)_{max} \leq 0.150$$

$$(R)_{le} \leq 0.0065$$

$$8.00º \leq (\Theta)_{te} \leq 16.0º \qquad (15)$$

$$C_{L1} \leq C_L \leq C_{L2}$$

$$C_{h1} \leq C_h \leq C_{h2}$$

$$C_p \leq -0.835$$

By posing the problem in these terms the optimisation is performed mainly at Mach 0.78, since the weighting factor is 0.9. The second point entails one constraint for Cp at Mach 0.20.

It must be pointed out that –4.0 deg is not the negative stall angle of attack, but a negative value sufficient to generate HTP Cp peaks, but small enough not to cause the flow calculation to fail. This point is important because one has to take into account that not only the reference geometry is going to be calculated by using the

OPTWIN code but also the 'perturbed' geometries during the optimisation process. If the design point is near the flow solver limits it is sure that the 'perturbed geometries' are going to be beyond, causing the optimisation design process to fail.

Some designed geometries were obtained taking one new design as the initial geometry for the next. It is worth noting that in the initial point there is one constraint violated, namely that corresponding to the minimum Cp. The initial design point is outside of the feasibility region. In the first design iterations, the code forces the result into the feasibility region, and once it is inside, it optimises the geometry. Usually the cost function increases during this process, although it did not happen in this case. Figure 8 represents the evolution of the cost function in the design process, where twelve design cycles were performed.
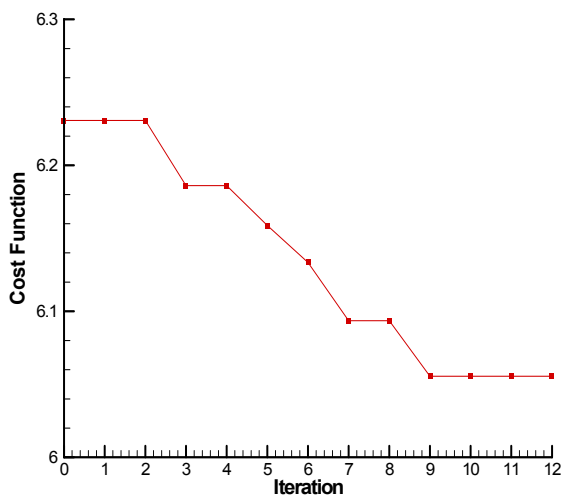
Fig. 8. Cost function evolution during the design process. HTP D17.4 test case.

The final designed geometry is called *HTP D17.4*. The results present some drag saving at high-speed regime although it is not so high than for the previous case. Figure 9 presents the drag polar comparison for Mach number 0.78 and Mach number 0.82.

For Mach number 0.78 there is a drag saving of 1.3 DC (based on the HTP reference surface):

Reference HTP:

$M_1 = 0.78, \mathrm{Re} = 16.9 \cdot 10^6, \alpha = -1.45°$

$C_L = -0.142$

HTP D17.4

$M_1 = 0.78, \mathrm{Re} = 16.9 \cdot 10^6, \alpha = -1.53°$

$C_L = -0.142$
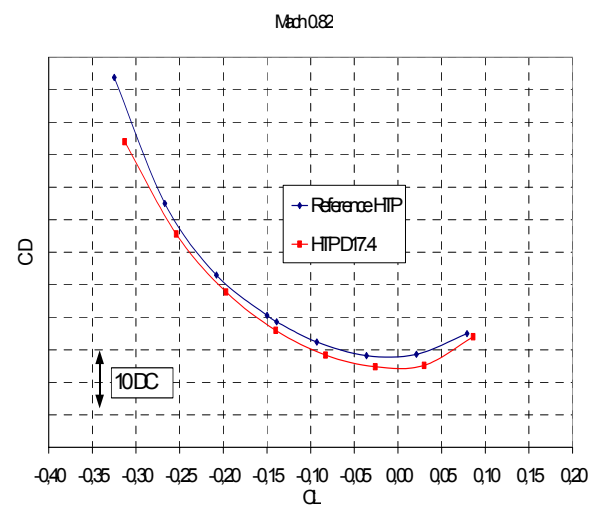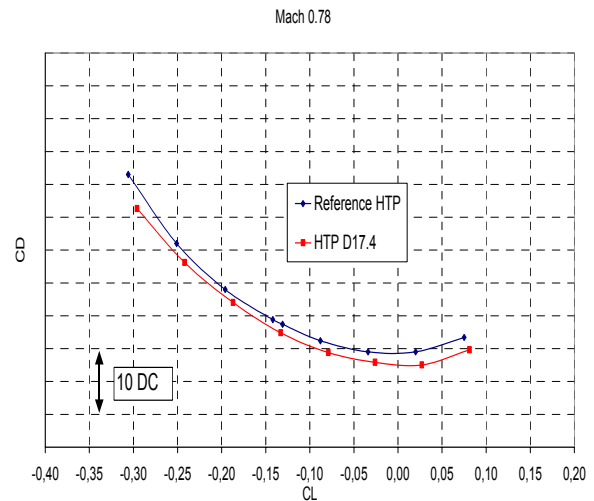
Fig. 9. Drag polar comparison between the reference HTP and the HTP D17.4. (Reference Surface = S_{HTP} = 31 m^2).

For Mach number 0.82 there is a drag saving of 1.4 DC (based on the HTP reference surface):

Reference HTP:

$M_2 = 0.82, \mathrm{Re} = 16.9 \cdot 10^6, \alpha = -1.45°$

$C_L = -0.150$

HTP D17.4

$$M_2 = 0.82, \mathrm{Re} = 16.9 \cdot 10^6, \alpha = -1.55°$$
$$C_L = -0.150$$

In the reference geometry the minimum Cp on the HTP is –0.975, whereas for the D17.4 design it is of –0.834, for almost the same C_L:

Reference HTP:
$$M_1 = 0.20, \mathrm{Re} = 12.6 \cdot 10^6, \alpha = -4.0°$$
$$C_L = -0.319, C_{p\min} = -0.975$$
HTP D17.4
$$M_1 = 0.20, \mathrm{Re} = 12.6 \cdot 10^6, \alpha = -4.0°$$
$$C_L = -0.317, C_{p\min} = -0.834$$
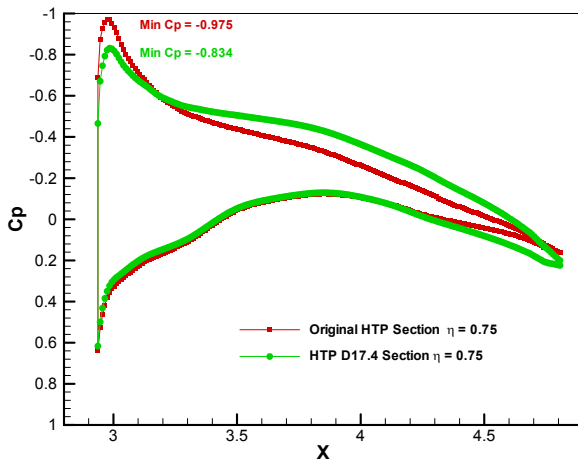
Fig. 10. Cp distribution comparison at span section η=0.75 between the reference HTP and the HTP D17.4. (Reference Surface = S_{HTP} = 31 m^2).

Figure 10 presents the Cp peak reduction for the section at 75% of span at Mach number of 0.20 and C_L=-0.319, where the minimum Cp along the HTP is located.

For positive angles of attack the Cp peak is also reduced:

Reference HTP:
$$M_1 = 0.20, \mathrm{Re} = 12.6 \cdot 10^6, \alpha = 2.0°$$
$$C_L = 0.178, C_{p\min} = -2.290$$

HTP D17.4
$$M_1 = 0.20, \mathrm{Re} = 12.6 \cdot 10^6, \alpha = 2.0°$$
$$C_L = 0.179, C_{p\min} = -1.930$$

4.4 Assessment of the designed and reference geometries

The use of a fast method of calculation within the optimisation loop is recommended. Nevertheless, several flow features, like flow separation, can not be predicted by this type of method. It is therefore necessary to assess with high fidelity flow solvers the trends in the HTP aerodynamics predicted by the optimiser. The confirmation of the trends enhances the level of confidence in the design method.

This is not exactly what is presented herein, because in this case the HTP has been analysed installed into the aircraft. The effect of installation can be very important and may also change the drag savings and other characteristics obtained for the isolated HTP. In fact, the last two steps of the design process –as shown in figure 3- have been gathered.

If an improvement of aerodynamic features is not confirmed, computations of the isolated and installed HTP should be carried out in order to assess the interference effects.

For the test cases shown in this paper, the datum and the new geometries have been evaluated installed in one Body + Tails model in order to compare the high speed and the low speed characteristics. The effect of the downwash span wise distribution due to the fuselage is in this way taken into account, whereas the wing effect is modeled by an average downwash angle. This span-wise downwash distribution due to the fuselage acts as an additional aerodynamic twist on the HTP, changing the inflow conditions.

The comparison between the new designs and the datum have been performed at the same model angle of attack and at the corresponding HTP setting angle to give the same HTP lift coefficient. Note that in this kind of model, the angle of attack value is intended to represent the inflow conditions in the rear part of the aircraft. It must be equal to the actual aircraft angle of attack minus the downwash angle.

In this analysis high fidelity codes have been used. For high speed the DLR RANS *Tau* code was employed [18], whereas for low speed analysis VSAERO was selected [19].

4.4.1 High-speed assessment

Figure 11 presents a picture of the computational mesh employed in the calculation. It is a hybrid mesh containing $3.7 \cdot 10^6$ nodes; 32 prismatic layers have been created to capture the boundary layer flow.

The calculations were performed at Mach numbers 0.78 and 0.82, depending on the case, and at flight Reynolds number ($18.6 \cdot 10^6$ based on the HTP AMC). The flow has been considered fully turbulent and the 1-equation Spallart-Almaras turbulence model has been used.
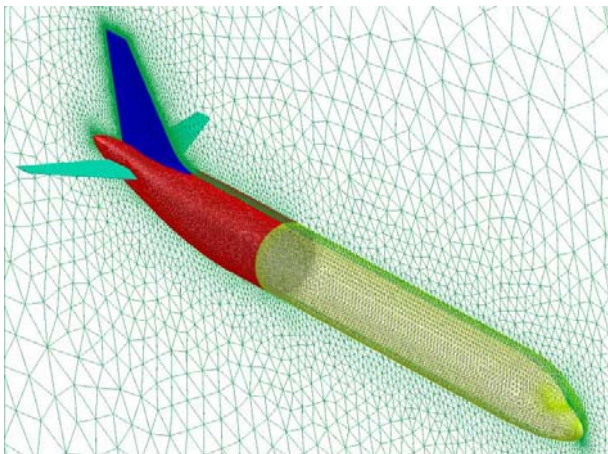
Fig. 11. Surface mesh for the computations at high speed with the Tau Flow Solver

4.4.1.1 HTP Optimal Twist Design

The HTP Optimal Twist design has been evaluated at $M = 0.78$, $C_{Lh} = 0.070$ (*cruise*).

For this condition a drag saving of 1.70 DC (based on the aircraft reference surface) has been achieved.

Note that a medium transport aircraft presents about 200 DC at cruise conditions. This feature can be exploited to achieve important drag reductions by only modifying the HTP.

4.4.1.2 HTP D9

Two conditions at high speed were considered for the design of this configuration. These conditions correspond to:

$$M = 0.78, C_{Lh} = 0.070 \ (cruise)$$

$$M = 0.82, C_{Lh} = 0.090$$

For the HTP D9 at Mach number of 0.78 (cruise condition) a drag saving of 0.66 DC is obtained (based on the aircraft reference surface).

For Mach number 0.82 (high speed cruise condition) no drag saving is obtained, but a small penalty of 0.27 DC (based on the aircraft reference surface).

Installation effects may contribute to reduce the predicted drag savings for the isolated HTP. At Mach number 0.82 a small drag increase appears. Nevertheless for normal cruise conditions, Mach number 0.78, there is a decrease in drag. Bearing in mind that the thickness-to-chord ratio of these airfoils is higher than the original, and a lighter structure could be designed, the results can be considered acceptable.

4.4.1.3 HTP D17.4

The design HTP D17.4 has been obtained by optimising the geometry at high speed regime and posing a very restrictive constraint at low speed, namely that for the minimum Cp.

For Mach number 0.78 there is a drag penalty of 2.07 DC (based on the aircraft reference surface).

For Mach number 0.82 there is a drag penalty of 3.81 DC (based on the aircraft reference surface).

Although an increase in drag has been obtained (more than 1% for a typical aircraft) one has to take into account that the datum did not fulfil all the constraints, e.g. that corresponding to the minimum Cp. The design point was outside the feasible region. The new design do verify all the constraints, it is a feasible solution.

In this case OPTWIN predicted a decrease in drag as it is shown in figure 9, but this little saving was lost when assessed the HTP with installation effects. A computation of the isolated HTP with Tau code would help to evaluate the contribution of the interference effects; but, this is out of the scope of the present paper.

In order to assess the advantages of this design it is also necessary to evaluate the Cp peak at low speed. A reduction for high negative angles of attack can be expected, because of the fulfilment of the minimum Cp constraint. Under these circumstances, it can be observed that imposing constraints and forcing the design to verify them is another way of improving one existing design.

4.4.2 Low Speed Assessment

The aim of this part is to assess the chord wise Cp distributions in the HTP for high negatives angles of attack at low speed for the Reference geometry and for the new design D17.4.This new HTP was designed by imposing a constraint at Mach number 0.20 in the value of the minimum Cp, and trying to reduce the drag at Mach number 0.78.
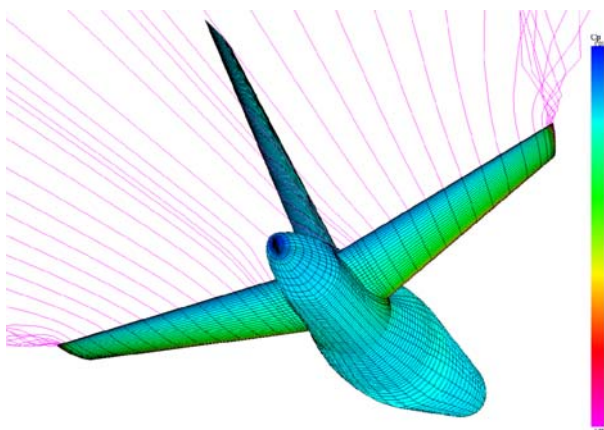
Figure 12. VSAERO model for the computations at low speed conditions.

This assessment has been performed with the VSAERO-code [19]. Figure 12 presents the model employed in these calculations.

Figure 13 presents the Cp chord wise distribution for two sections along the span, at 40% and at 75% of semi span, for the same C_{Lh} and for the Reference HTP and HTP D17.4. It can be seen how the Cp peak for negative angles of attack is highly reduced; this feature of the optimisation follows the same trend for the installed HTP than that of the isolated HTP.
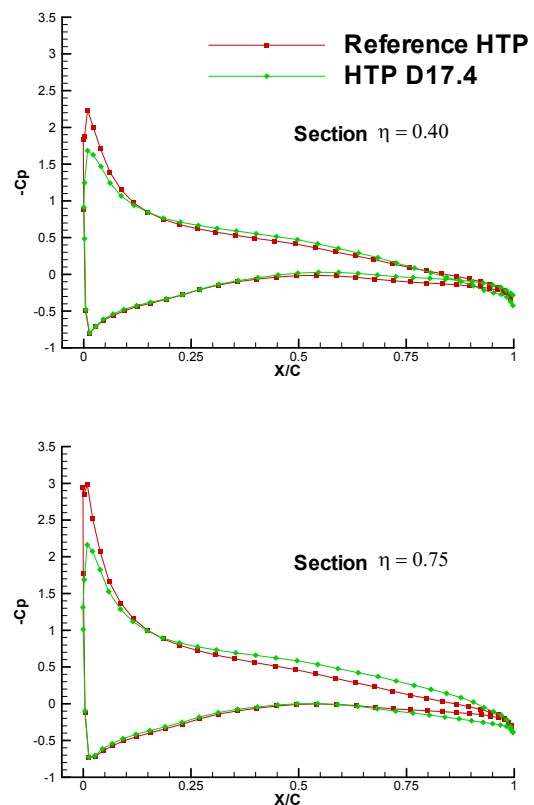
Figure 13. Comparison of Cp chord wise distributions for Reference HTP and HTP D17.4 at the same lift (C_{Lh}= -0.50). A reduction in the negative Cp peak is observed.

For this kind of airfoil a reduction in the negative Cp peak for the same C_L can lead to an increase in the stall angle of attack. While this parameter drives the tail sizing, a reduction in the HTP size could be undertaken. It is shown in this example how, although the aerodynamic drag at high speed has been increased under the fuselage and other effects – chapter 4.4.1.3- the fulfilment of a constraint can make a design acceptable. In multidisciplinary scenery, both the proper election of the cost function and of the

requirements have to be used to represent a real design problem.

5 Conclusions

A 3-D design code based on a constrained numerical optimisation method has been developed at INTA to perform preliminary design of wings and horizontal tailplanes. The code performs a design at a low computational cost. New designs for the horizontal tailplane of a medium size transport aircraft were carried out. The resultant geometries were then installed into the fuselage to take into account interference effects and then analysed with high fidelity flow solvers. An improvement of the tailplane and aircraft performances can be achieved. These results show the reliability of this type of tool for wing/HTP design and its usefulness for eliminating unnecessary steps in the iterative design process.

6 Acknowledgements

References

[1] A.Van der Velden, R. Kelm, D. Kokan, J.Mertens. Application of MDO to Large Subsonic Transport Aircraft. *AIAA-2000-0844*, pp.11, 2000.

[2] J. L. Walsh, J.C. Townsend, A.O. Salas, J.A.Samareh, V. Mukhopadhyay, J.-F. Barthelemy. Multidisciplinary High-Fidelity Analysis and Optimization of Aerospace Vehicles, Part 1: Formulation. *AIAA-2000-0418*, pp. 1-17, 2000.

[3] J. L. Walsh, R.P.Weston, J.A.Samareh, B. H. Mason, L.L. Green, R.T. Biedron. Multidisciplinary High-Fidelity Analysis and Optimization of Aerospace Vehicles, Part 2: Preliminary Results. *AIAA-2000-0419*, pp. 1-21, 2000.

[4] F. Kafyeke, M. Abdo, F. Pépin, P.Piperni, E. Larendeau. Challenges of Aircraft Design Integration. *Reduction of Military Vehicle Acquisition Time and Cost throughAdvanced Modelling and Virtual Simulation (RTO Conference)*, París, France, 48, pp 1-10, 2002.

[5] D. Quagliarella. Aerodynamic Design of Classical and Innovative Configurations Using a Hybrid Asymmetric Multiobjective Algorithm. *Ercoftac Design Optimisation: Methods and Applications*, Athens, Greece, 2004.

[6] V.Selmin, P.L. Vitagliano, A.Pennavaria and L. Crossetta. Alenia Multidisciplinary Design Optimisation-Topics and Approaches. *Aerodynamic Design and Optimisation of Flight Vehicles in a Concurrent Multi-disciplinary Environment (RTO Conference)*, Ottawa, Canada, 20, pp 1-7, 1999.

[7] M.Orlowski, W. Tang. A System for the Aerodynamic Optimisation of Three-Dimensional Configurations. *Aerodynamic Design and Optimisation of Flight Vehicles in a Concurrent Multi-disciplinary Environment (RTO Conference)*, Ottawa, Canada, 19, pp 1-12, 1999.

[8] D. Sasaki, G. Yang, S. Obayashi. Automated Aerodynamic Optimization System for SST Wing-Body Configuration. *AIAA-2002-5549*, pp 1-9, 2002.

[9] Jiménez-Varona J. An inverse method for transonic wing design. *International Journal for Numerical Methods in Engineering*, No. 44, pp 249-264, 1999.

[10] Monge F., Jiménez-Varona J. Design and Optimisation of Wings in Transonic Regime. *Aerodynamic Design and Optimisation of Flight Vehicles in a Concurrent Multi-disciplinary Environment (RTO Conference)*, Ottawa, Canada, 21, pp 1-10, 1999.

[11] F. Monge and F. Palacios. Aerodynamic Multipoint Airfoil Optimization using Control Theory on unstructured meshes, *4th European Congress on Computational Methods in Applied Sciences and Engineering (ECCOMAS)* , Jyväskylä (Finland), pp 1-20, 24th-28th July 2004.

[12] Vanderplaats, G.N. CONMIN-a Fortran Program for Constrained Function Minimization, User´s Manual. *Technical Report TM X-62,282*, NASA, 1978.

[13] Arora J.S. *Introduction to Optimum Design*. 1st edition, McGraw-Hill, Inc, 1989.

[14] W. Press, W. Vetterling, S. Taukolsky, B. Flannery. *Numerical Recipes in FORTRAN, the Art of Scientific Computing*. Cambridge University Press, 1992.

[15] Jiménez-Varona J. Computations of DFVLR-F4 model using a viscous flow solver for transonic wings. *Technical Report AT/TNO/4510/001/INTA/98,* INTA, 1998.

[16] Yang Q.-Z., Wichmann G. Calculation of transonic wing flow by interaction of a potential and an integral three dimensional laminar-turbulent boundary layer method. *Technical Report IB 129-98/11, DLR*, 1998.

[17] Ruiz-Calavera L., Hiroshe N. Parametric Studies of a time-accurate finite-volume Euler code in the NWT Parallel computer. *Progress and Challenges in CFD Methods and Algorithms (AGARD Conference)*, Seville, Spain, 38, pp 1-10, 1995.

[18] DLR. Tau-Code User Guide. Revision 1.24. 2003.

[19] J.K. Nathman, *VSAERO* A Computer Program for Calculating the Nonlinear Aerodynamic Characteristics of Arbitrary Configurations. *Users′ Manual.Version 6.2*. Release Date: June 2001